ACS APPLIED MATERIALS & INTERFACES

Research Article

www.acsami.org

Single Macroscopic Pillars as Model System for Bioinspired Adhesives: Influence of Tip Dimension, Aspect Ratio, and Tilt Angle

Maurizio Micciché,[†] Eduard Arzt,[†,‡] and Elmar Kroner*[,§]

[†]INM – Leibniz Institute for New Materials, Functional Microstructures Group, Campus D2 2, 66123 Saarbrücken, Germany

[‡]Saarland University, 66123 Saarbrücken, Germany

[§]INM – Leibniz Institute for New Materials, Switchable Surfaces Group, Campus D2 2, 66123 Saarbrücken, Germany

Supporting Information

ABSTRACT: The goal of our study is to better understand the design parameters of bioinspired dry adhesives inspired by geckos. For this, we fabricated single macroscopic pillars of 400 μm diameter with different aspect ratios and different tip shapes (i.e., flat tips, spherical tips with different radii, and mushroom tips with different diameters). Tilt-angle-dependent adhesion measurements showed that although the tip shape of the pillars strongly influences the pull-off *force*, the pull-off *strength* is similar for flat and mushroom-shaped tips. We found no tilt-angle dependency of adhesion for spherical tip structures and, except for high tilt angle and low preload experiments, no tilt-angle effect for mushroom-tip pillars. For flat-tip pillars, we found a strong influence of tilt angle on adhesion, which decreased linearly with increasing aspect ratio. The experiments show that for the tested aspect ratios between 1 and 5, a linear decrease of tilt-angle dependency is found. The results of our studies will help to design bioinspired adhesives for application on smooth and rough surfaces.

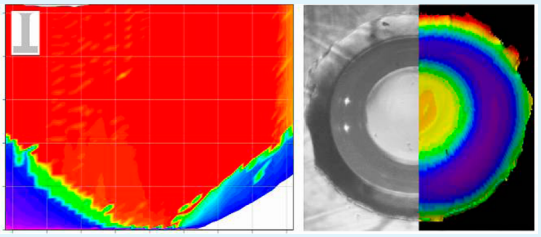

KEYWORDS: *gecko, adhesion, PDMS, angle, pillar, microstructure*

1. INTRODUCTION

Due to their extraordinary climbing abilities, geckos have become the subject of many studies. They can climb on nearly every kind of surface, which has been explained as a result of the complex surface structures on their toes.[1−5] The adhesion system of geckos combines unique properties such as high and reversible adhesion, rapid residue-free detachment, and anisotropic adhesion performance.[5−7] Thus, the natural system has been mimicked in order to transfer the effect found in nature into applications.[8−13] Much effort has been spent to understand the biological system, to artificially fabricate gecko-inspired surface structures, and to systematically vary geometrical parameters. The most commonly fabricated surface patterns are usually arrays of pillars in the micro- and nanometer range.[14−16] Various studies revealed that the adhesive properties of such patterned surfaces depend on the shape,[13,17−19] size,[16] and aspect ratio[16,20] of the pillars.

However, most of these measurements were performed using a spherical probe[16,21,22] or a flat probe without controlled alignment.[23] In our previous work, we showed that both cases may lead to results which do not describe the adhesive properties of patterned surfaces correctly.[24] For example, spherical probe testing causes contact formation with an increasing number of pillars with increasing preload;[22,24] the pillars at the boundary of the contact area experience tilt. We have previously shown that this may lead to an underestimate of the adhesive properties of patterned surfaces.[24] Other experiments showed that increasing the pillar aspect ratio (AR, defined as height divided by diameter) results in an increasing pull-off force.[16,20] However, pillars with higher AR have a lower effective Young's modulus. Thus, at identical preload, more pillars will attach to the spherical probe for high AR structures compared to low AR ones. This would lead to a larger number of pillars in contact and thus to a higher pull-off force, which is caused by the probe geometry but not by the adhesive performance of the pillars.[24] Finally, it is known that the tip shape strongly influences the adhesive properties,[13] but the mechanism is difficult to isolate as the shape of the spherical probe interferes with the tip shape.[25] In our earlier studies, we showed that many effects can be better investigated by testing single macroscopic pillars.[25,26] They allow a better control over the pillar geometry as well as in situ visualization and simple data analysis.[26] In this study, we therefore tested single, macroscopic pillars for their adhesion properties while changing geometric parameters and measurement conditions. We measured the adhesive properties of spherical, flat, and mushroom-shaped pillars with aspect ratios from 1 to 5. We investigated the tilt-angle-dependent adhesion, performed in situ visualization of the detachment, and applied advanced data analysis methods.[26]

Received: December 25, 2013
Accepted: April 29, 2014
Published: April 29, 2014

   dx.doi.org/10.1021/am405873j | ACS Appl. Mater. Interfaces 2014, 6, 7076−7083

2. EXPERIMENTAL SECTION

2.1. Fabrication and Characterization of Single Macropillars. Single macroscopic pillars were fabricated by molding of polydimethylsiloxane (PDMS, Sylgard 184, Dow Corning) from aluminum templates (Figure 1). The templates contained a cavity 10 mm in diameter and 3 mm in depth, with a milled hole in the center. Each template had a hole with a diameter d of 400 μm and different lengths l ranging from 400 μm up to 2000 μm. PDMS was mixed with a prepolymer to cross-linker ratio of 10:1, degassed in a desiccator, filled into the templates, and degassed again until no bubbles formed above the milled hole. After curing the samples in air for 2 h at 75 °C, pillars with flat tips were achieved. This resulted in PDMS single macroscopic pillars with diameters of 400 μm and aspect ratios (AR), defined as l/d, of 1, 2, 3, 4, and 5.

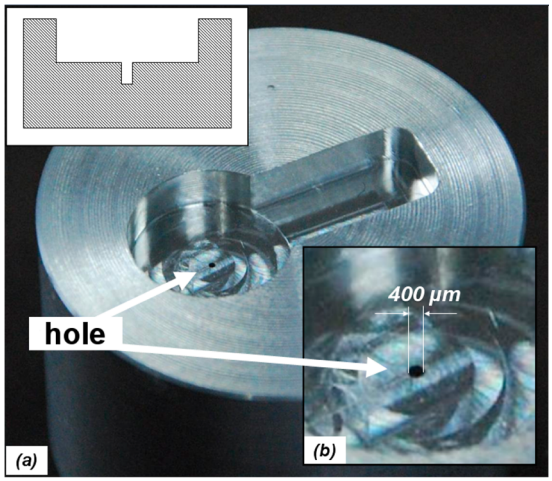

Figure 1. (a) Template with milled hole of 400 μm diameter in the middle of a cavity. (b) Close-up image of the milled hole in the template.

Spherical and mushroom-shaped tips were fabricated as follows: Spherical tips were achieved by placing a droplet of uncured PDMS with a needle on the tip of a pillar. Because of the surface tension, a spherical cap formed which was then cured. To achieve mushroom-shaped tips, a small piece of glass was plasma-activated in an oxygen environment and put into a 10 wt % solution of hexamethyldisilazane and cyclohexane for 10 h. Afterward, a liquid droplet of PDMS was placed on top of a flat-tip pillar, similar as for obtaining spherical tips, but was then squashed with the silanized glass piece. Different heights of the spherical tips and different widths of the mushroom shaped tips were achieved by varying the amount of PDMS placed on top of the pillars. The modified pillars were cured in air at 75 °C for 16 h. Afterward, the thin glass was carefully removed from the mushroom-shaped tips. All samples were characterized using white light interferometry and optical microscopy. Pillars with flat tips were taken as references for the diameter d and the length l (Figure 2a). The height of the spherical tips h was determined by subtracting the height of the reference pillars with the same AR from the height of the spherical pillars. The radius of curvature r of the spherical tips was calculated by assuming the tip to be a segment of a sphere, using $r = (h^2+a^2)/2h$, with a being the radius of the pillar ($d/2$) (Figure 2b). The width w of mushroom shaped tips was measured by optical microscopy (Figure 2c).

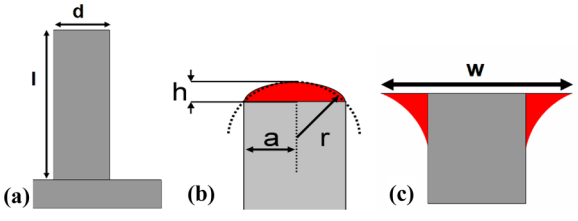

Figure 2. (a) Flat pillar with diameter d and length l. (b) Spherical tip with height h, radius a, and radius of curvature r. (c) Mushroom-shaped tip with width w.

2.2. Adhesion Measurements. Adhesion was measured using the macroscopic adhesion measurement device.[27] It allows adhesion experiments with defined tilt angle, pull-off speed, and preload. All measurements were performed with silicon wafers as probes. The probes were pressed against the specimens and pulled off at a constant velocity of 10 μm/s while measuring the forces. The maximum compressive force and tensile force are defined as preload and pull-off force. The following parameters were varied:

(1) Tip geometry: pillars with spherical, flat, and mushroom-shaped tips were investigated
(2) Preload: all samples were measured with a wide range of preload.
(3) Tilt angle: the tilt angle was varied from −2.0° and +2.0° with respect to the aligned position in 0.1° steps.

Prior to all measurements, the probe was brought into contact a few hundred times with PDMS to obtain an equilibrium surface state.[28] Also, the pillars were aligned perpendicularly to the probe as described elsewhere.[25]

Videos were recorded in situ with a frame rate of 25 pictures per second and a resolution of 720 × 546 pixels. The resolution was approximately 10 μm in the $x-y$ direction. Video recording started in the noncontact mode, recording contact formation and detachment. The videos are given in Supporting Information.

3. RESULTS

3.1. Characterization of the Pillars. The measured dimensions of the different pillars are listed in Table 1.

Table 1. Dimensions of Pillars[a]

	flat		spherical			mushroom	
nominal AR	l (μm)	d(μm)	l(μm)	h(μm)	r(μm)	l(μm)	w(μm)
1	418	395	556	138	210	418	611
			486	69	317	419	707
2	760	398	862	102	245	762	760
			840	80	288	762	780
3	1168	393	1324	156	202	1169	655
			1235	67	323	1169	747
4	1553	411	1662	109	248	1555	706
			1632	79	307	1555	801
5	1941	408	2062	121	233	1942	635
			2020	79	303	1942	738

[a]Maximum error lies within ±5 μm.

3.2. Influence of Tip Geometry and Preload on Adhesion. Figure 3 shows the pull-off force as a function of preload measured on AR 3 pillars with different tip geometries. The mushroom-shaped pillar exhibits the highest pull-off force (~20 mN), followed by the flat-tip pillar (~7.4 mN) and the spherical tip pillar (~180 μN). Each pillar, independent of tip shape and AR, reaches its maximum pull-off force at small preloads; further increase in preload resulted only in a small change in pull-off force.

3.3. Influence of Aspect Ratio on Adhesion. The pull-off forces for flat-tip pillars with different AR are plotted as a function of preload in Figure 4. The pull-off forces lie between 5 and 8 mN. No systematic influence of AR can be identified. However, pillars which show lower pull-off force values at low preload exhibit a slight preload dependency of the pull-off force.

dx.doi.org/10.1021/am405873j | ACS Appl. Mater. Interfaces 2014, 6, 7076−7083

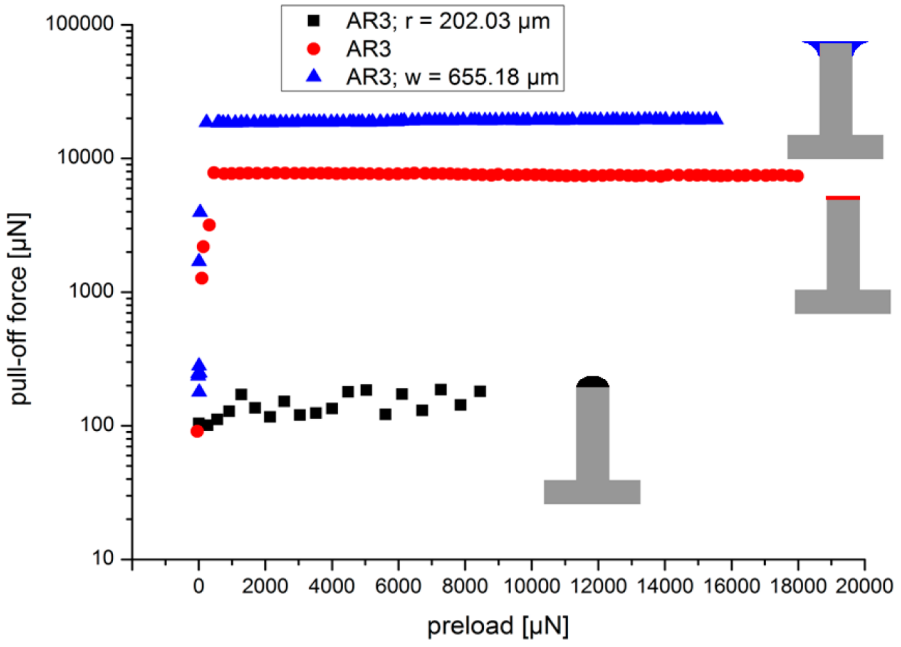

Figure 3. Influence of tip shape on pull-off force as a function of preload, measured on pillars with AR 3. The average pull-off force (P_c) and pull-off strength (calculated by dividing force by the pillar area) (σ_c) are for spherical tip (r = 202 μm) structures 141 ± 6 μN and 1.12 ± 0.05 kPa, for flat-tip structures 7580 ± 16 μN and 60.0 ± 0.1 kPa, and for mushroom tip (w = 655 μm) structures 19093 ± 36 μN and 152.0 ± 0.2 kPa, respectively.

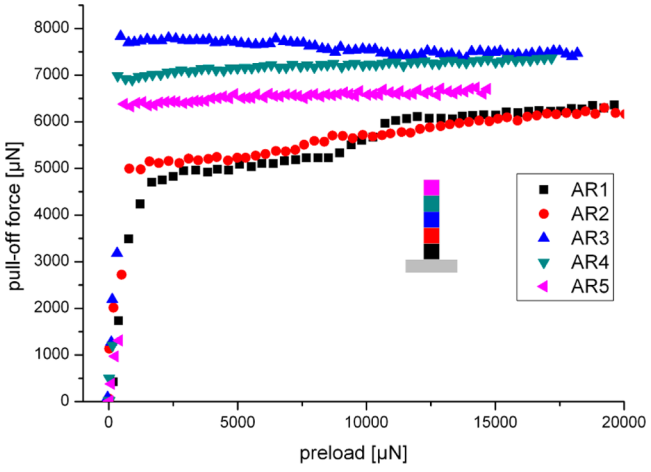

Figure 4. Pull-off force as a function of preload for pillars with flat tips and different AR. The lowest pull-off force is found for AR 1 and AR 2, the highest pull-off force is found for AR 3. The pull-off force values are very similar and no systematic influence of the AR on the pull-off force is found. With increasing preload, the pull-off force values converge.

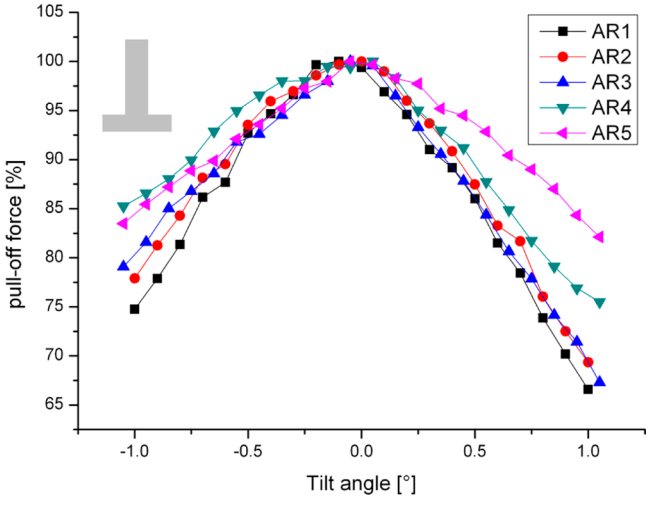

Figure 5. Pull-off force of flat-tip pillars with different AR as a function of tilt angle. All samples show decreasing pull-off force with increasing tilt angle. The tilt-angle dependency is higher for lower AR.

For high preload, the pull-off forces are very similar and lie within 6 and 8 mN pull-off force.

3.4. Influence of AR on Tilt-Angle-Dependent Adhesion for Flat Tip Pillars. Figure 5 shows the pull-off force of flat-tip pillars with different AR as a function of tilt angle. The pull-off force is normalized with respect to the maximum pull-off force at 0° tilt angle for better comparison and was measured at a preload of 20 mN. With increasing tilt angle, the pull-off force decreases. This decrease shows a slight dependency on AR, the low AR pillars having smaller opening angles compared to the high AR pillars. The slight asymmetry of the curves is caused by imperfection of the samples.

3.5. Influence of Tilt Angle on Adhesion. Figure 6 shows representative tilt-angle-dependent pull-off force measurements for flat (Figure 6a), spherical (Figure 6b), and mushroom-tip pillars (Figure 6c). The resulting pull-off force is color coded, with red representing high pull-off values and blue/violet depicting low pull-off values.

Pillars with flat tips showed the highest tilt-angle dependence of the pull-off force. In the aligned state, the pull-off force is independent of the applied preload. Small misalignment resulted in a significant decrease in pull-off force (Figure 6a). For very low preload and high tilt angle, adhesion became very low. Video analysis showed that the applied preload was then not sufficient for full contact formation. The pull-off force of spherical tip pillars was not angle dependent (Figure 6b). Note

dx.doi.org/10.1021/am405873j | ACS Appl. Mater. Interfaces 2014, 6, 7076−7083

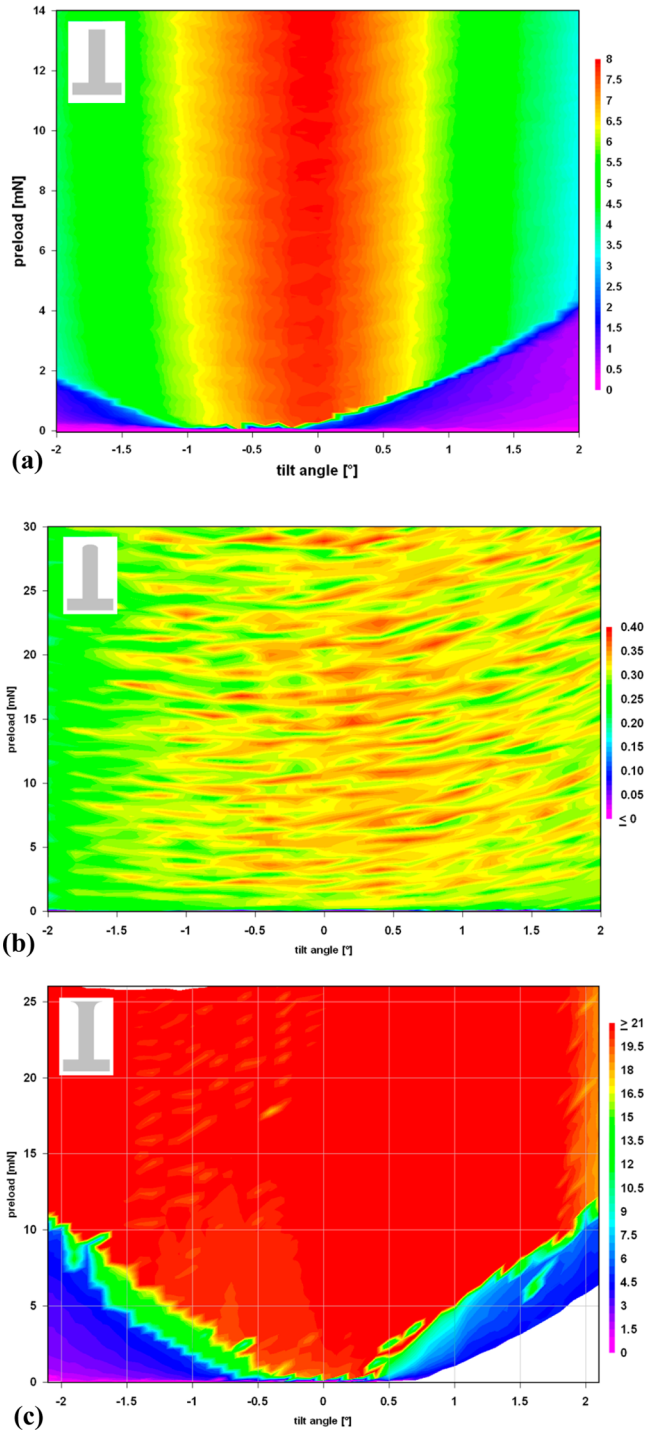

Figure 6. Influence of the tilt angle on the pull-off force. The *x*-axis shows the tilt angle with respect to the aligned position, and the *y*-axis corresponds to the applied preload. The pull-off force is color coded. (a) Flat tip pillar, where small changes in tilt angle results in a significant drop in pull-off force; (b) spherical tip pillar, where the pull-off force remains constant over the measured angle range; and (c) mushroom-tip pillar, where the pull-off force is angle-dependent only for small preload and high tilt angle.

that the pattern is an artifact caused by the noise of the system due to the low pull-off forces.

Mushroom-shaped pillars showed an angle dependent pull-off force only for high tilt angles and small preload (Figure 6c). Similar to the flat pillar case, the very low pull-off forces at low preload and high tilt angle were associated with incomplete contact found in the video analysis. At high preload the pull-off force leveled out and reached a maximum for all mushroom-shaped samples.

3.6. Influence of Tip Dimensions on Adhesion. The pull-off forces for spherical tip pillars with varying radius of curvature and different mushroom diameters are shown in Figure 7a,b. For the spherical tips, a higher radius of tip curvature leads to an increase in pull-off force. For the mushroom-tip pillars, the pull-off force increases with increasing tip width. No systematic AR dependency is found.

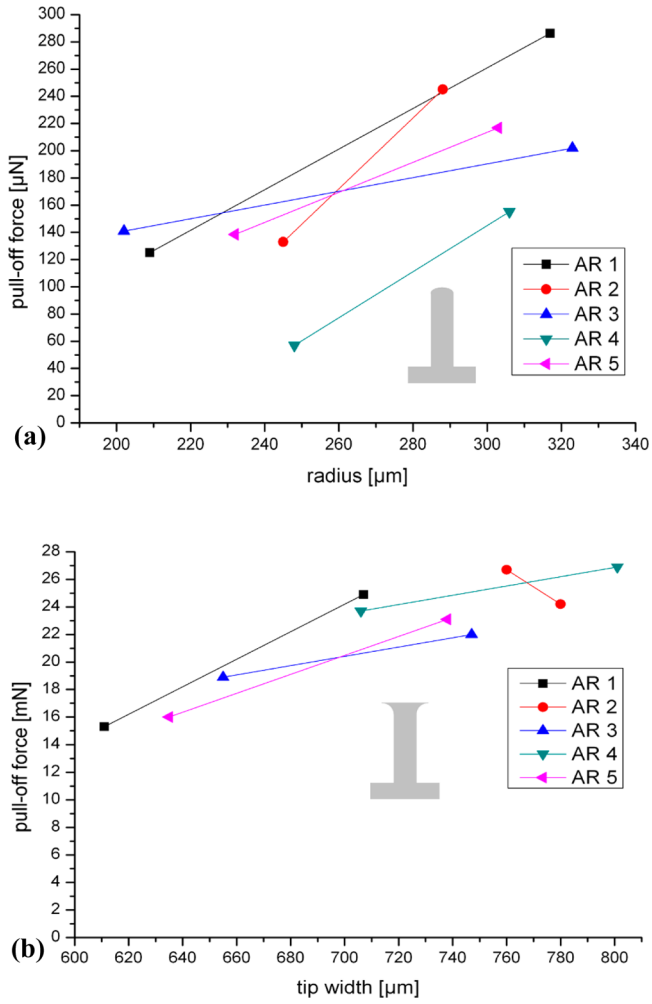

Figure 7. Influence of the tip geometry on adhesion. (a) Pull-off force increases with increasing radius of curvature *r* for spherical tip pillars. (b) Pull-off force increases with increasing tip-width *w* for mushroom-tip pillars. No apparent influence of aspect ratio is found.

4. DISCUSSION

Our experiments on pillars with different tip geometry confirm the adhesion trend found for micropillars[13] and macropillars[25] (see Figure 3). Pillars with mushroom-shaped tips show adhesion values increased by a factor of about 3 compared to flat-tip pillars. Both flat and mushroom-tip structures exhibit more than 100 times higher adhesion compared to spherical tip structures. Note that this comparison is done for the pull-off force but not for the true pull-off strength taking the real contact area into account. The determination of the pull-off

dx.doi.org/10.1021/am405873j | ACS Appl. Mater. Interfaces 2014, 6, 7076−7083

strength for the spherical tip structure is difficult. However, if the forces are divided by the pillar area (apparent pull-off strength of the pillars), the forces will show the same ratio as the strengths. Thus, in the case of our single pillar experiments, the pull-off forces can be directly compared with each other.

Earlier studies on micropillars have concluded that the AR has a significant influence on adhesion[16] (i.e., the pull-off force increases with increasing AR). Our results in Figure 4 indicate that there is no systematic AR effect. It may be argued that the two lowest AR samples show the lowest adhesion, but a clear trend cannot be identified. Further, the difference between the pull-off forces for different AR becomes less pronounced for high preloads. This can be explained as small defects on the pillar surfaces may be of less importance if the preload is high enough to flatten them out. In our earlier study, we already suggested that the AR effect found for microstructures using spherical probes may be due to the testing geometry.[25] If a spherical probe indents an array of micropillars with flat tips, the pillars in the boundary region of the contact area form only partial contact or experience a tilt angle. In Figure 6a,c, it can be seen that for partial contact of a pillar (high misalignment, low preload), the adhesive force is reduced to very low values and becomes negligible. For flat-tip pillars, the pull-off force also depends on the tilt angle (Figure 6a), where an increase in misalignment leads to a significant loss in adhesion. Only if the pillars are very compliant can they adapt to the spherical probe and contribute to adhesion. Figure 5 shows the tilt-angle-dependent pull-off force for flat-tip structures. The structure with the lowest AR shows the highest tilt-angle dependency of adhesion. With increasing AR, the tilt-angle dependency becomes less pronounced. For better comparability, the intermediate slope for all AR in the range of +0.5 to +1.0° and from −1.0 to −0.5° are plotted in Figure 8. A high number

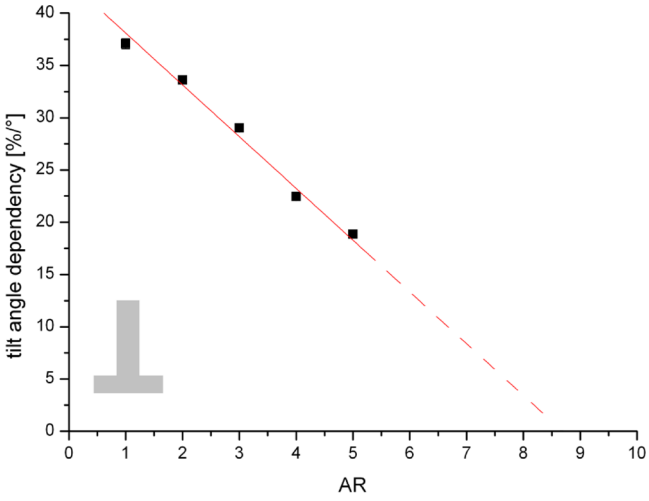

Figure 8. Slopes from Figure 5 for the range of +0.5° to +1.0° and from −1.0° to −0.5° as a function of AR. A high number represents a high tilt-angle-dependent adhesion. With increasing AR, the tilt-angle dependency becomes less pronounced.

indicates a high tilt-angle dependency. The experimental error lies within the symbol size. It can be clearly seen that the pull-off force becomes less angle-dependent with increasing AR. Interestingly, the change in tilt-angle dependency seems to be linear for the tested AR. A linear extrapolation to a tilt-angle dependency of 0 suggests that for a given material and pillar geometry there is a critical aspect ratio of ∼9, where no tilt-angle dependency is found for flat-tip structures. However, it is more likely that at a certain AR, the tilt-angle dependency deviates from this linear trend. As high AR structures tend to collapse due to attractive forces between the structures, these values become irrelevant for experimental studies.

Both the tilt-angle dependency of the pull-off force and the AR effect for flat-tip pillars can be explained by the stress states within the pillars. With increasing tilt angle and decreasing AR, the stresses at the edge between pillar and probe increase. This leads to a preferential initiation of a detachment crack, which subsequently leads to low adhesion. This effect is important especially for flat-tip structures, where the highest stress is located at the edge of the contact. Spherical-tip pillars have a symmetrical contact zone. Also, the mushroom shape ensures that the maximum stress zone is located not at the edge of the contact area but somewhere in the middle.[19] Thus, neither for spherical nor for mushroom-tip structures is a strong angle dependency or AR influence expected, which we found in our results (Figure 5c).

Our experiments also give insight into how the detachment mechanism leads to high adhesion. For spherical tip structures, the adhesion increases with increasing tip radius. This is to be expected from various contact theories between spherical bodies.[29] For this geometry, the detachment can be considered as a contact, which is notched on two sides. Slight tensile forces on the pillar will drive the detachment front further and will eventually lead to detachment at low forces. This explains the low pull-off forces found for spherical tip pillars in Figures 3 and 7a.

For the flat-tip structure, there is a void present in the middle of the structure during contact (Figure 9a). This is due to the shape of the pillar tip. Figure 9b shows a white light interferometry picture of the pillar tip. *Note that the white light interferometry picture is not to scale*; the cavity in the middle has a depth of <9 μm, which is less than 2% compared to the diameter of 400 μm. The material within this small dimple will not be in contact before detachment occurs. Nevertheless, shortly prior to detachment, a detachment crack forms at the edge of the flat-tip structure and propagates to the middle of the structure (Figure 9a). A video of the adhesion test is given in the Supporting Information.

For the mushroom-tip structures, the detachment starts in the middle of the contact area, as shown in the in situ picture in Figure 9c. After the initiation, the detachment front is driven further until only the flap is in contact (Figure 9d). Finally, the flap also detaches. The full sequence is given in the Supporting Information. Detachment initiation in the middle of the mushroom-shaped tip is to be expected, as the tensile stress at the contact edge goes to low values due to the shape.[30] Figure 9e shows the topography of the mushroom-shaped tip. The dimple was filled during the tip fabrication process, leading to the opposite geometry (i.e., having a slight bump in the middle of the contact area).

The pictures in Figure 9 and the videos of the adhesion experiments (see Supporting Information) suggest that there may be a suction effect present, as predicted theoretically[17] and shown experimentally.[31−33] Especially, the detachment behavior of the mushroom-shaped pillar tip is interesting, as it occurs in two steps. First, a circular detachment area is initiated in the middle of the contact area, but the detachment crack seems to stop at a certain radius. Then, the mushroom flap suddenly detaches. This behavior is in contrast to the behavior reported for microstructures which were monitored with a high speed

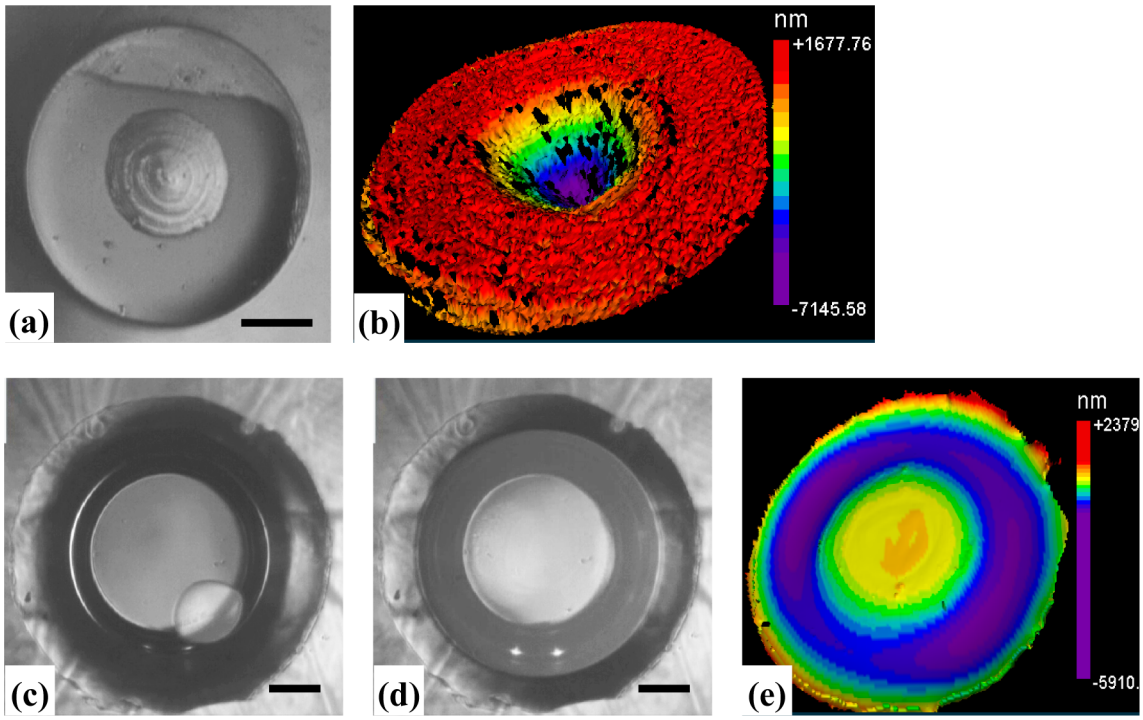

Figure 9. Tip snapshots of adhesion experiments and pillar tip geometries. (a) Flat-tip pillar during initiation of detachment; the detachment is initiated at the edge (top of the picture) and propagates to the center. The dimple in the middle is due to the fabrication process of the mold. (b) White light interferometry picture of the pillar tip, showing the 9 μm deep dimple caused by the milling process in the mold. (c) Initiation of detachment for a mushroom-tip pillar, which can be seen as a bubble-like appearance in the lower right edge. (d) Detachment of the inner part of the mushroom-tip pillar. The mushroom flap is still in contact. (e) White light interferometry picture of the mushroom tip. The scale bar in panels (a), (b), and (d) corresponds to 100 μm. For video files, see Supporting Information.

camera.[34] The reason for this discrepancy may be due to the different strain rates; the micropillar experiments in the reported publication had a height of approximately 100 μm and experienced a strain of 50 μm/s, equivalent to 50% strain per second for the micropillars. The present pillars had a height up to 2 mm and were loaded with 10 μm/s, or 0.005% strain per second. It may also be possible that the maximum strain before detachment was larger for the micropillar study. To clarify the mechanism further, a multiscale experiment is necessary to test all structure sizes with comparable velocities and at a high frame rate, which will be the scope of future studies.

The pull-off strength was calculated for the flat-tip and mushroom-tip pillar by dividing the measured pull-off force by the tip area of the pillars. Figure 10 shows the pull-off strength as a function of tip width, assuming its diameter as the tip width for the flat-tip pillar. Interestingly, the flat-tip and mushroom-tip structures have similar pull-off strength values of approximately 50−70 kPa. This indicates that the pull-off force may not be directly determined by the tip shape for the tested macropillars. Also, the pull-off force is not directly influenced by the detachment mechanism, because detachment is initiated from the contact boundary for the flat-tip pillar but in the middle of the contact area for the mushroom pillars. One possible explanation for this behavior is that the pillars are too large for having strong tip-shape dependence. It is much more likely that the detachment is defect-controlled[35] and, due to the large dimensions of the contact area, has similar failure loads for the flat and mushroom shaped pillars. In contrast to micropillars,[13] the tip shape of macroscopic pillars is less significant to achieve high adhesion, as long as the real contact

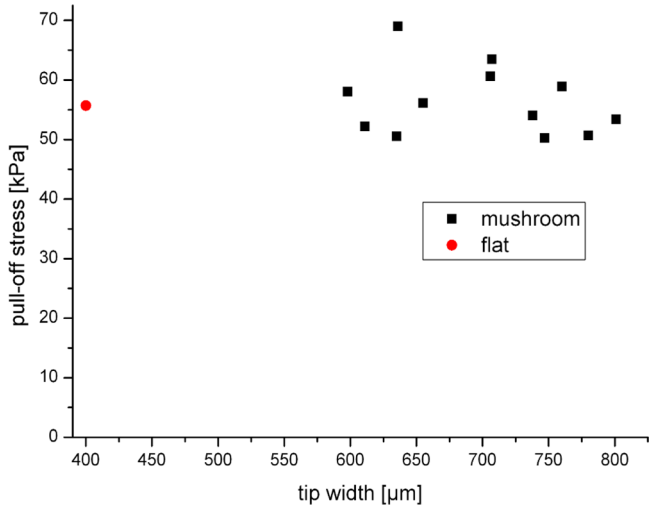

Figure 10. Adhesion strength as a function of tip width for the mushroom- and flat-tip pillars.

area is comparable (i.e., the packing density of the flat-tip pillars is higher to compensate for the smaller tip area).

5. CONCLUSIONS

Our experiments on macroscopic single pillars with different tip shapes have, on one hand, confirmed several existing results, but give, on the other hand, new insights and even questions existing results in the field of bioinspired dry adhesives. The results can be summarized as follows: (1) For tip shape, our measurements have shown that the tip shape is of importance

as known from other studies.[13] Mushroom-shaped pillars show higher pull-off forces compared to flat-tip pillars or spherical-tip pillars. However, for the flat and mushroom structures, the pull-off strength values are comparable, if the complete contact area is considered. The pull-off force of mushroom tips with different diameters scales with their tip width. The reason for this behavior might be caused by additional suction effects, which are to be expected for structures with this size. On the other hand, it has to be experimentally proven if this effect exists only for large macroscopic pillars, or also for micro- and nanopillars. (2) For aspect ratio, we did not find any clear influence of the aspect ratio, as reported earlier.[16] The discrepancy of results in literature may be caused by the testing geometry. In earlier studies, mainly spherical probes were used. Thus, the effective Young's Modulus determines the maximum contact area for a given preload. For lower effective Young's Modulus, the contact area would be higher, leading to higher adhesion. (3) For tilt angle, we found similar tilt-angle effects as in previous publications[25] (i.e., no tilt effect for spherical tip structures, tilt effect at low preload and high tilt angle for mushroom tips, and high tilt effect for flat-tip pillars). For the first time we showed that the aspect ratio has a strong influence on the tilt-angle-dependent adhesion of flat-tip structures. With increasing aspect ratio, the tilt-angle dependency of adhesion decreases. The decrease in tilt-angle dependency follows a linear trend.

■ ASSOCIATED CONTENT

Supporting Information

Video of attachment and detachment for a flat-tip pillar and video of attachment and detachment of a mushroom-shaped pillar. This material is available free of charge via the Internet at http://pubs.acs.org.

■ AUTHOR INFORMATION

Corresponding Author

*E-mail: elmar.kroner@inm-gmbh.de. Tel.: +49 (0) 681/9300369.

Notes

The authors declare no competing financial interest.

■ REFERENCES

(1) Autumn, K.; Liang, Y. A.; Hsieh, S. T.; Zesch, W.; Chan, W. P.; Kenny, T. W.; Fearing, R.; Full, R. J. Adhesive Force of a Single Gecko Foot-Hair. *Nature* **2000**, *405*, 681−685.

(2) Gorb, S. Biological Microtribology: Anisotropy in Frictional Forces of Orthopteran Attachment Pads Reflects the Ultrastructure of a Highly Deformable Material. *Proc. R. Soc. B* **2000**, *267*, 1239−1244.

(3) Autumn, K.; Peattie, A. M. Mechanisms of Adhesion in Geckos. *Integr. Comp. Biol.* **2002**, *42*, 1081−1090.

(4) Autumn, K.; Sitti, M.; Liang, Y. A.; Peattie, A. M.; Hansen, W. R.; Sponberg, S.; Kenny, T. W.; Fearing, R.; Israelachvili, J. N.; Full, R. J. Evidence for Van der Waals Adhesion in Gecko Setae. *Proc. Natl. Acad. Sci. U.S.A.* **2002**, *99*, 12252−12256.

(5) Arzt, E.; Gorb, S.; Spolenak, R. From Micro to Nano Contacts in Biological Attachment Devices. *Proc. Natl. Acad. Sci. U.S.A.* **2003**, *100*, 10603−10606.

(6) Hiller, U.; Blaschke, R. Zum Haftproblem der Gecko-Fusse. *Naturwissenschaften* **1967**, *54*, 344−345.

(7) Arzt, E. Biological and Artificial Attachment Devices: Lessons for Materials Scientists from Flies and Geckos. *Mater. Sci. Eng., C* **2006**, *26*, 1245−1250.

(8) Sathya, C.; John, T.; Kimberly, T. A Microfabricated Gecko-Inspired Controllable and Reusable Dry Adhesive. *Smart Mater. Struct.* **2013**, *22*, 025013.

(9) Jin, K.; Tian, Y.; Erickson, J. S.; Puthoff, J.; Autumn, K.; Pesika, N. S. Design and Fabrication of Gecko-Inspired Adhesives. *Langmuir* **2012**, *28*, 5737−5742.

(10) Boesel, L. F.; Greiner, C.; Arzt, E.; del Campo, A. Gecko-Inspired Surfaces: A Path to Strong and Reversible Dry Adhesives. *Adv. Mater.* **2010**, *22*, 2125−2137.

(11) Murphy, M. P.; Aksak, B.; Sitti, M. Gecko-Inspired Directional and Controllable Adhesion. *Small* **2009**, *5*, 170−175.

(12) Northen, M. T.; Greiner, C.; Arzt, E.; Turner, K. L. A Gecko-Inspired Reversible Adhesive. *Adv. Mater.* **2008**, *20*, 3905−3909.

(13) Del Campo, A.; Greiner, C.; Arzt, E. Contact Shape Controls Adhesion of Bioinspired Fibrillar Surfaces. *Langmuir* **2007**, *23*, 10235−10243.

(14) Cheung, E.; Sitti, M. Adhesion of Biologically Inspired Polymer Microfibers on Soft Surfaces. *Langmuir* **2009**, *25*, 6613−6616.

(15) Jeong, H. E.; Suh, K. Y. Nanohairs and Nanotubes: Efficient Structural Elements for Gecko-Inspired Artificial Dry Adhesives. *Nano Today* **2009**, *4*, 335−346.

(16) Greiner, C.; del Campo, A.; Arzt, E. Adhesion of Bioinspired Micropatterned Surfaces: Effects of Pillar Radius, Aspect Ratio, and Preload. *Langmuir* **2007**, *23*, 3495−3502.

(17) Spolenak, R.; Gorb, S.; Gao, H.; Arzt, E. Effects of Contact Shape on the Scaling of Biological Attachments. *Proc. R. Soc. A* **2005**, *461*, 305−319.

(18) Soto, D.; Hill, G.; Parness, A.; Esparza, N.; Cutkosky, M.; Kenny, T. Effect of Fibril Shape on Adhesive Properties. *Appl. Phys. Lett.* **2010**, *97*, 053701.

(19) Spuskanyuk, A. V.; McMeeking, R. M.; Deshpande, V. S.; Arzt, E. The Effect of Shape on the Adhesion of Fibrillar Surfaces. *Acta Biomater.* **2008**, *4*, 1669−1676.

(20) Aksak, B.; Hui, C. Y.; Sitti, M. The Effect of Aspect Ratio on Adhesion and Stiffness for Soft Elastic Fibres. *J. R. Soc., Interface* **2011**, *8*, 1166−1175.

(21) Aksak, B.; Murphy, M. P.; Sitti, M. Adhesion of Biologically Inspired Vertical and Angled Polymer Microfiber Arrays. *Langmuir* **2007**, *23*, 3322−3332.

(22) Crosby, A. J.; Hageman, M.; Duncan, A. Controlling Polymer Adhesion with "Pancakes. *Langmuir* **2005**, *21*, 11738−11743.

(23) Davis, C. S.; Martina, D.; Creton, C.; Lindner, A.; Crosby, A. J. Enhanced Adhesion of Elastic Materials to Small-Scale Wrinkles. *Langmuir* **2012**, *28*, 14899−14908.

(24) Kroner, E.; Paretkar, D.; McMeeking, R.; Arzt, E. Adhesion of Flat and Structured PDMS Samples to Spherical and Flat Probes: A Comparative Study. *J. Adhes.* **2011**, *87*, 447−465.

(25) Kroner, E.; Arzt, E. Single Macropillars as Model Systems for Tilt Angle Dependent Adhesion Measurements. *Int. J. Adhes. Adhes.* **2012**, *36*, 32−38.

(26) Kroner, E.; Arzt, E. Mechanistic Analysis of Force-Displacement Measurements on Macroscopic Single Adhesive Pillars. *J. Mech. Phys. Solids* **2013**, *61*, 1295−1304.

(27) Kroner, E.; Blau, J.; Arzt, E. Note: An Adhesion Measurement Setup for Bioinspired Fibrillar Surfaces Using Flat Probes. *Rev. Sci. Instrum.* **2012**, *83*, 016101.

(28) Kroner, E.; Maboudian, R.; Arzt, E. Adhesion Characteristics of PDMS Surfaces During Repeated Pull-Off Force Measurements. *Adv. Eng. Mater.* **2010**, *12*, 398−404.

(29) Johnson, K. L.; Kendall, K.; Roberts, A. D. Surface Energy and the Contact of Elastic Solids. *Proc. R. Soc. A* **1971**, *324*, 301−313.

(30) Carbone, G.; Pierro, E.; Gorb, S. N. Origin of the Superior Adhesive Performance of Mushroom-Shaped Microstructured Surfaces. *Soft Matter* **2011**, *7*, 5545−5552.

(31) Davies, J.; Haq, S.; Hawke, T.; Sargent, J. P. A Practical Approach to the Development of a Synthetic Gecko Tape. *Int. J. Adhes. Adhes.* **2009**, *29*, 380−390.

(32) Heepe, L.; Varenberg, M.; Itovich, Y.; Gorb, S. N. Suction Component in Adhesion of Mushroom-Shaped Microstructure. *J. R. Soc., Interface* **2011**, *8*, 585−589.
(33) Sameoto, D.; Sharif, H.; Menon, C. Investigation of Low-Pressure Adhesion Performance of Mushroom Shaped Biomimetic Dry Adhesives. *J. Adhes. Sci. Technol.* **2012**, *26*, 2641−2652.
(34) Heepe, L.; Kovalev, A. E.; Filippov, A. E.; Gorb, S. N. Adhesion Failure at 180 000 Frames per Second: Direct Observation of the Detachment Process of a Mushroom-Shaped Adhesive. *Phys. Rev. Lett.* **2013**, *111*, 104301.
(35) Kamperman, M.; Kroner, E.; del Campo, A.; McMeeking, R. M.; Arzt, E. Functional Adhesive Surfaces with "Gecko" Effect: The Concept of Contact Splitting. *Adv. Eng. Mater.* **2010**, *12*, 335−348.